# Tectonic re-interpretation of the Banggai-Sula–Molucca Sea margin, Indonesia

IAN M. WATKINSON*, ROBERT HALL & FARID FERDIAN

*SE Asia Research Group, Department of Earth Sciences, Royal Holloway University of London, Egham, Surrey TW20 0EX, UK*

**Corresponding author (e-mail: i.watkinson@es.rhul.ac.uk)*

**Abstract:** High resolution multibeam bathymetric and seismic data from the area north of the Banggai-Sula Islands, Indonesia, provide a new insight into the geological history of the boundary between the East Sulawesi ophiolite, the Banggai-Sula microcontinent and the Molucca Sea collision zone. Major continuous faults such as the Sula Thrust and the North Sula–Sorong Fault, previously interpreted to bound and pass through the area are not seen. The south-verging Batui Thrust previously interpreted offshore to the east of Poh Head cannot be identified. In the areas where the thrust was interpreted there is a north-vergent thrust and fold zone overlain by almost undeformed sediments. Gently dipping strata of the Banggai-Sula microcontinent margin can be traced northwards beneath younger rocks. In the east, rocks of the Molucca Sea collision complex are deformed by multigenerational folds, thrusts and strike-slip faults. There is a series of small thrusts between the leading edge of the collision complex and the foot of the slope. In the west a zone of transpression close to the East Arm of Sulawesi is the termination of the dextral strike-slip Balantak Fault extending east from Poh Head.

The Banggai-Sula microcontinent or block (Fig. 1) lies to the east of the East Arm of Sulawesi in eastern Indonesia within the complex triple junction between the Pacific, Australian and Eurasian plates. Stratigraphic similarities between the microcontinent and the Australian continent led to the idea that it originated from western Irian Jaya (e.g. Audley-Charles *et al.* 1972; Hamilton 1979) or further east in Papua New Guinea (Pigram *et al.* 1985; Garrard *et al.* 1988). It has become a well established concept that the microcontinent was sliced from the Australian northern continental margin in New Guinea and travelled westwards (e.g. Visser & Hermes 1962; Hamilton 1979; Silver & Smith 1983; Pigram *et al.* 1985; Garrard *et al.* 1988) along the Sorong Fault, possibly coupled to the Philippine Sea Plate (Ali & Hall 1995; Hall *et al.* 1995; Hall 1996).

The Banggai-Sula microcontinent's westward movement was arrested by collision with the East Arm of Sulawesi but the timing is debated. It is generally thought to have occurred in the Neogene (Simandjuntak & Barber 1996) but a range of ages has been suggested including Miocene (Hamilton 1979), Early to Middle Miocene (Bergman *et al.* 1996), Middle Miocene (Sukamto & Simandjuntak 1983; Simandjuntak 1986), Middle Miocene to Pliocene (Garrard *et al.* 1988), and Late Miocene (Silver *et al.* 1983; Davies 1990; Smith & Silver 1991; Parkinson 1998).

During the collision, ophiolites were obducted and thrust eastwards over the microcontinent, to form an imbricate collision zone at the east end of the East Arm of Sulawesi (e.g. Kündig 1956; Silver *et al.* 1983; Simandjuntak 1986; Davies 1990; Simandjuntak & Barber 1996). Compressional deformation of the Banggai-Sula microcontinent itself, including reactivation of Mesozoic structures on land in the Sula Islands, has also been interpreted by Garrard *et al.* (1988) to have resulted from the NW-directed (Hamilton 1979; Silver *et al.* 1983) collision.

Although the microcontinent is small, the results of its collision are often considered to extend significantly beyond the immediate zone of orogenesis. Westward thrusting of the central Sulawesi metamorphic belt, a foreland fold and thrust belt in west Sulawesi, magmatism in west Sulawesi, and deformation in the Makassar Strait and Borneo have all been attributed to the collision (e.g. Coffield *et al.* 1993; Bergman *et al.* 1996; Simandjuntak & Barber 1996; Pubellier *et al.* 1999*a*; Calvert 2000; McClay *et al.* 2000). Today there is a mountain range over 3000 m high immediately west of the collision zone exposing the ophiolite which remains difficult to explore and as little studied as it was when described by Brouwer (1925) and Rutten (1927).

Most studies have been aimed at understanding the tectonic development of the collisional orogen

*From*: Hall, R., Cottam, M. A. & Wilson, M. E. J. (eds) *The SE Asian Gateway: History and Tectonics of the Australia–Asia Collision*. Geological Society, London, Special Publications, **355**, 203–224.
DOI: 10.1144/SP355.10 0305-8719/11/$15.00 

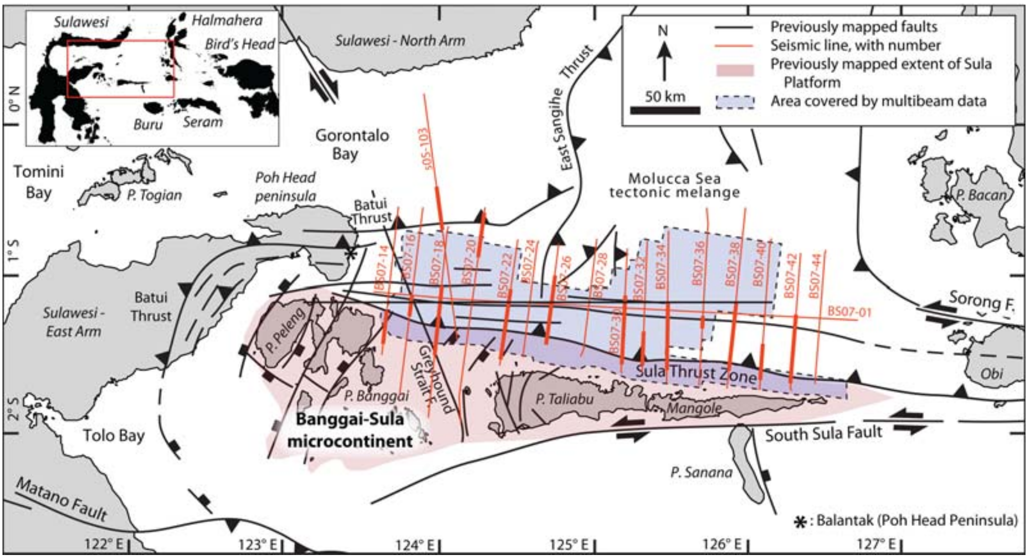


**Fig. 1.** Map showing the location of the study area, the Banggai-Sula microcontinent (pink) and principal tectonic features identified in previous studies. Faults modified after Silver *et al.* (1983); Garrard *et al.* (1988). Red lines are seismic lines, shown in bold for sections illustrated in subsequent figures; the blue area is the extent of multibeam data. Note that structures in this map are quite different from those we now propose in Figure 15.

on Sulawesi and at the western end of the Banggai-Sula microcontinent, but little attention has been paid to the northern margin of the Banggai-Sula microcontinent. Silver *et al.* (1983) produced maps based on a range of geophysical and field observations, acquired particularly from marine cruises, showing the position of faults, and these, together with the work of Hamilton (1979), have formed the basis for much subsequent work (Fig. 1). However, since the early 1980s there have been relatively few new observations made in the offshore region around the Banggai-Sula microcontinent. Recently, some new seismic and multibeam bathymetric data have been acquired. This paper presents a structural interpretation based largely on these new data from the area north of the Banggai-Sula microcontinent and the southern Molucca Sea, and some new field observations on land, which provide the basis for a better understanding of the significance of the structures and their regional context.

## Tectonic setting

East Sulawesi and the Banggai-Sula microcontinent are presently sutured along the Batui Thrust zone (Fig. 1), which accommodated much of the shortening between the two regions during Neogene collision (e.g. Kündig 1956; Hamilton 1979; McCaffrey *et al.* 1981; Silver *et al.* 1983; Simandjuntak 1986; Beaudouin *et al.* 2003). It is widely considered to be bounded by strands of the Sorong Fault system. A southern strand of the Sorong Fault, called the South Sula–Sorong Fault was interpreted by Hamilton (1979) to follow the break in slope south of Taliabu and pass between Mangole and Sanana (Fig. 1). The dramatic increase in water depth south of this line suggests that the area is floored by oceanic crust, supported by dredging and marine geophysical observations in the North Banda basin (e.g. Hinschberger *et al.* 2000), and therefore the fault marks the southern margin of the Banggai-Sula microcontinent. The South Sula–Sorong Fault (Fig. 1) is a splay of the strike-slip fault which can be traced east to Irian Jaya, and which is interpreted to have facilitated the left-lateral westward translation of the Banggai-Sula microcontinent (e.g. Hamilton 1979; Sukamto & Simandjuntak 1983; Hall 1996; Simandjuntak & Barber 1996; Villeneuve *et al.* 2002; Beaudouin *et al.* 2003). It is often shown to link, via the Matano Fault, to the Palu-Koro Fault of central Sulawesi, sinistral structures which ultimately connect to subduction at the North Sulawesi trench, suggesting clockwise rotation of the block north and east of these faults (e.g. Hamilton 1979; Silver *et al.* 1983; Walpersdorf *et al.* 1998; Stevens *et al.* 1999; Socquet *et al.* 2006).

North of the Banggai-Sula microcontinent, other strands of the Sorong Fault have been mapped. The North Sula–Sorong Fault is traced by Hamilton (1979) from the Bird's Head peninsula, south of Obi, along the north of the Banggai-Sula Islands, and towards Poh Head and is shown in slightly different positions by other authors (e.g. Norvick 1979; Silver *et al.* 1983; Sukamto & Simandjuntak 1983). Australian continental crust is known from SW Obi (Wanner 1913; Ali & Hall 1995) although most of the island is ophiolite suggesting a splay may pass through Obi. However, no geological evidence of significant strike-slip faulting has been recorded on Obi, and there is little geophysical evidence for the fault in this position. Another strand of the Sorong Fault is interpreted to pass north of Obi and south of Bacan, called the Molucca–Sorong Fault by Hamilton (1979) and may continue towards Gorontalo Bay to the west (Fig. 1). Beneath Gorontalo Bay well located hypocentres (Engdahl *et al.* 1998) show an abrupt termination of the west-subducting Molucca Sea Plate suggesting that a strand of the Sorong Fault may be traced from south of Bacan into Gorontalo Bay along a line trending about 285° (Cottam *et al.* 2011).

Thrusts observed south of the North Sula–Sorong Fault by Silver *et al.* (1983) have been named the Sula Thrust and interpreted to form a continuous north-dipping thrust zone. North of the North Sula–Sorong Fault, almost 10 cm/a convergence between the Philippine Sea and Eurasian Plates is largely accommodated by the Sangihe and Halmahera thrusts, which lie above the double subduction zone in the Molucca Sea (e.g. Silver & Moore 1978; McCaffrey *et al.* 1980; Moore & Silver 1980; Hall 1987, 2002; Rangin *et al.* 1996; Pubellier *et al.* 1999*b*; Beaudouin *et al.* 2003). Sediments within this zone are being squeezed southwards, to form the Molucca Sea collision complex (Silver & Moore 1978; Silver *et al.* 1983).

Much of Sulawesi's present-day seismicity is associated with subduction of the Celebes Sea beneath the North Arm, and Molucca Sea subduction north of the Banggai-Sula microcontinent (Cardwell *et al.* 1980; Engdahl *et al.* 1998; Beaudouin *et al.* 2003). Scattered earthquakes occur outside of these areas throughout Sulawesi and the islands to the east, some of which may be associated with the major Sorong and Matano Faults, and GPS vectors have been interpreted in terms of fault-bounded blocks (Socquet *et al.* 2006). Very little shallow seismicity occurs immediately north of the Banggai-Sula microcontinent (Cardwell *et al.* 1980; Engdahl *et al.* 1998; Beaudouin *et al.* 2003) indicating that there are few active structures in this area, or that deformation is largely aseismic.

## Dataset

This study is based upon geophysical data acquired from the offshore area immediately north of Pulau Taliabu and Pulau Mangole, part of the Sula Islands east of Sulawesi, Indonesia (Fig. 1). Sixteen north–south-trending lines and one east–west-trending seismic line were acquired from January to March 2007 by the M/V Mezen as part of the IndoDeep–Banggai-Sula (BS07) Non Exclusive 2-D survey, on behalf of TGS. The data were recorded by Sercel SEAL instruments using a 3980 cu. in. Sodera G-Gun at 5 m depth with a 25 m shotpoint interval. The seismic data were filtered to remove external noise, de-multipled, and pre-stack time migrated.

During March–May 2007 the M/V L'Espoir acquired 40 746 km$^2$ of multibeam data in the same area of which about 22 000 km$^2$ is presented here. This 3D coverage was acquired using a Kongsberg Simrad EM120 Multibeam Echo Sounder using 191 beams at equidistant spacing. Positioning control used a C-Nav Starfire DGPS. During processing, positioning, tidal and calibration corrections were applied, random noise and artefacts were removed, and a terrain model using a 25 m bin size was gridded and exported to ESRI format. Multibeam data were further processed in ERMapper to remove voids and generate digital elevation models (DEMs) in which the azimuth of artificial lighting was rotated in 45° increments through 360° to illuminate features with different orientations. Images used in this paper are illuminated from the NW and in most a greyscale is used as it more clearly shows structural features.

The study area is composed of two distinct zones: in the south, north-dipping seabed (Fig. 2) is underlain by a series of parallel reflections which appear to be continuous with strata onshore in the Sula Islands. This slope area represents the northern margin of the Banggai-Sula microcontinent. From the foot of the slope to the northern extent of the dataset is the second zone, composed of complexly deformed sediments in water depths of $\geq$1 km. The relatively shallow, plateau-like, western and eastern parts of the deep area are separated by a deeper central area, and are described separately as the western and NE areas (Fig. 3).

## Stratigraphy

The Banggai-Sula Islands have a relatively simple stratigraphy (Garrard *et al.* 1988; Supandjono & Haryono 1993; Surono & Sukarna 1993). The basement is Palaeozoic or older metamorphic rocks intruded by Permo-Triassic granites associated with acid volcanic rocks. These rocks are overlain by undated, probably Lower Jurassic, terrestrial sediments and by Jurassic and Cretaceous marine shales and limestones. In the western parts of the islands are Eocene to Miocene and younger Neogene limestones. On Taliabu the basement rocks form an elevated core to the island with Mesozoic sediments dipping mainly to the north and south.

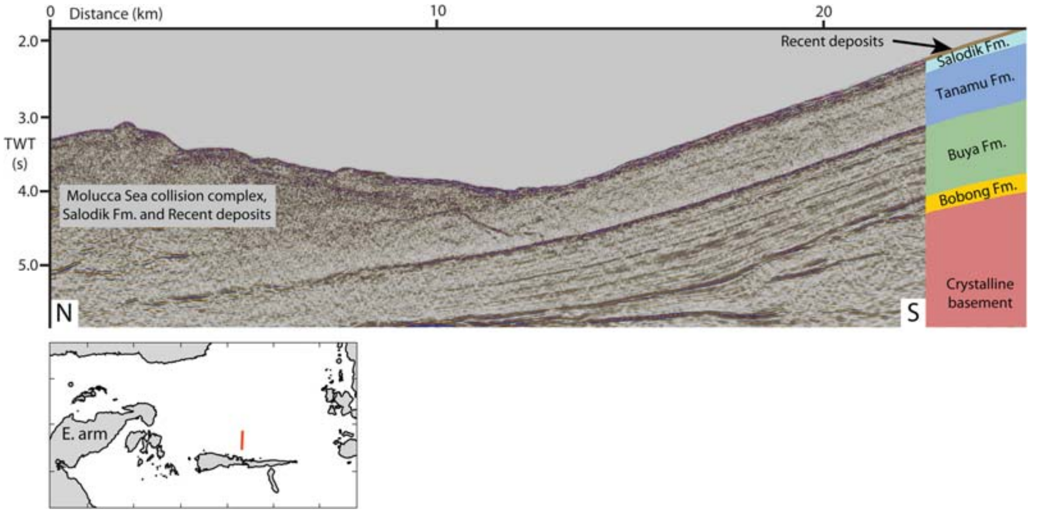


**Fig. 2.** Summary seismic stratigraphy drawn onto seismic line BS07-32. See inset map for location.

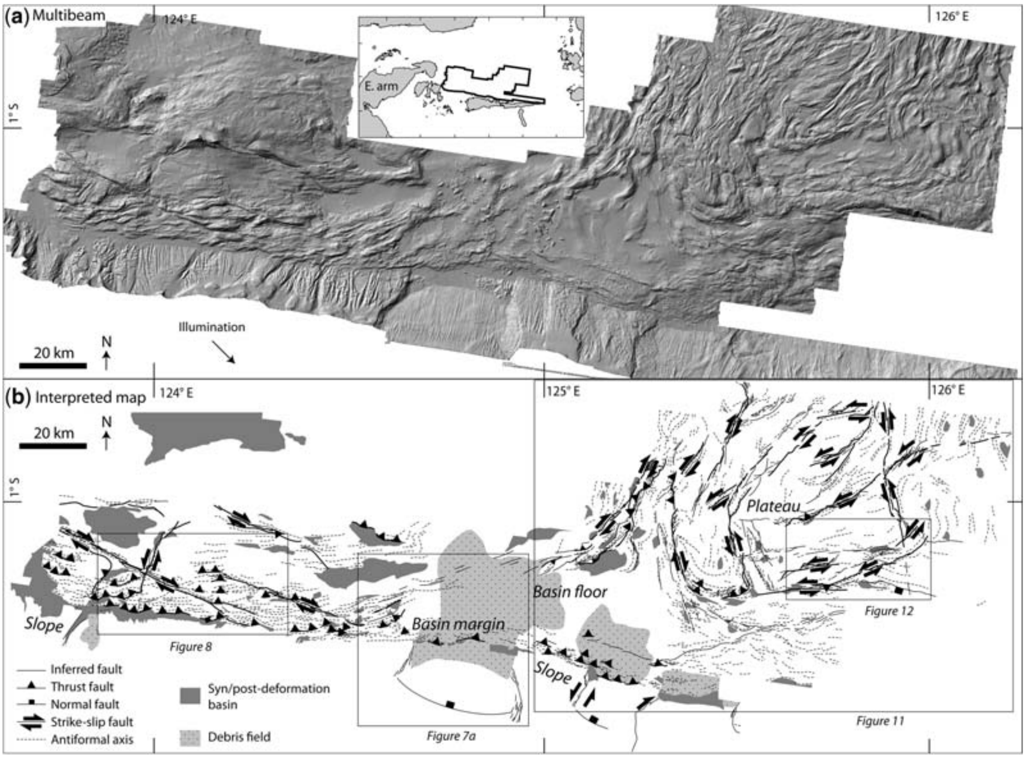


**Fig. 3.** (**a**) Shaded relief map of the multibeam data. See inset map for location. Illumination from the NW. (**b**) Interpreted structural map, showing fault kinematics, basin areas, and fields of debris derived from the collapsing slope in the south. Locations of subsequent figures shown.

## *Banggai-Sula margin stratigraphy*

The Banggai-Sula margin and slope is dominated by sub-parallel strata which dip gently north (Fig. 2), and appear to be continuous with Mesozoic sedimentary rocks exposed on Banggai, Taliabu and Mangole, immediately south of the study area. There are no offshore wells, and we have interpreted correlations between seismic packages identified offshore with rocks observed on land to the south.

The lowermost seismic package is largely structureless, and is likely to represent crystalline basement. This crops out onshore in the centre and around the southern edge of Taliabu and Banggai. It is composed of folded metasediments, marbles, schists, gneisses and amphibolites of probable Permo-Carboniferous age, intruded by granites and associated acid bodies of Permo-Triassic age (Supandjono & Haryono 1993).

Reflections above the basement, which appear to be fault-bounded, are interpreted to be terrestrial conglomerates and sandstones of the Lower Jurassic Bobong Formation within half graben, which rest unconformably on the basement onshore to the south (Garrard *et al.* 1988; Surono & Sukarna 1993). The strong acoustic contrast between this package and the widespread, onlapping seismic package above, are correlated with marine shales of the Middle–Upper Jurassic Buya Formation which overlie the Bobong Formation on land (Supandjono & Haryono 1993).

A thick, widespread and weakly reflective seismic package (Fig. 2) above the Buya Formation is interpreted to represent deepwater carbonates of the Cretaceous Tanamu Formation, which lies unconformably above the Buya Formation in the central part of the Sula Islands (Garrard *et al.* 1988; Supandjono & Haryono 1993; Surono & Sukarna 1993). Platform and reefal carbonates of the Eocene–Miocene Salodik and Pancoran Formations are widespread across eastern Sulawesi and the Banggai-Sula Islands (e.g. Rusmana *et al.* 1993; Supandjono & Haryono 1993; Surono & Sukarna 1993), and are represented by a package of strong, closely spaced reflections at the top of the slope stratigraphic sequence on the westernmost seismic lines (e.g. Fig. 4a).

## *Basin floor stratigraphy*

Most of the material of the basin floor is strongly deformed and lacks coherent seismic reflections. Much of it is almost certainly allochthonous (see discussion in the 'Basin margin' section).

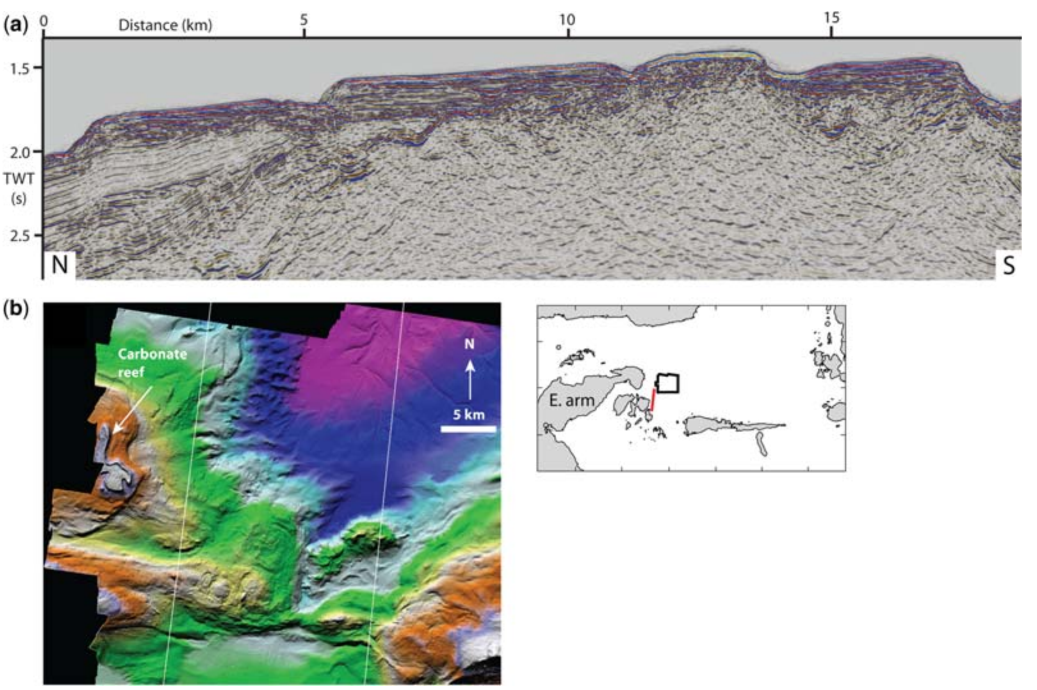


**Fig. 4.** (**a**) Detail from seismic line BS07-14 showing subsided carbonate platforms (note vertical scale at left). (**b**) Depth-coloured multibeam DEM showing well developed carbonate platform in plan view, close to the seismic line. See inset map for location.

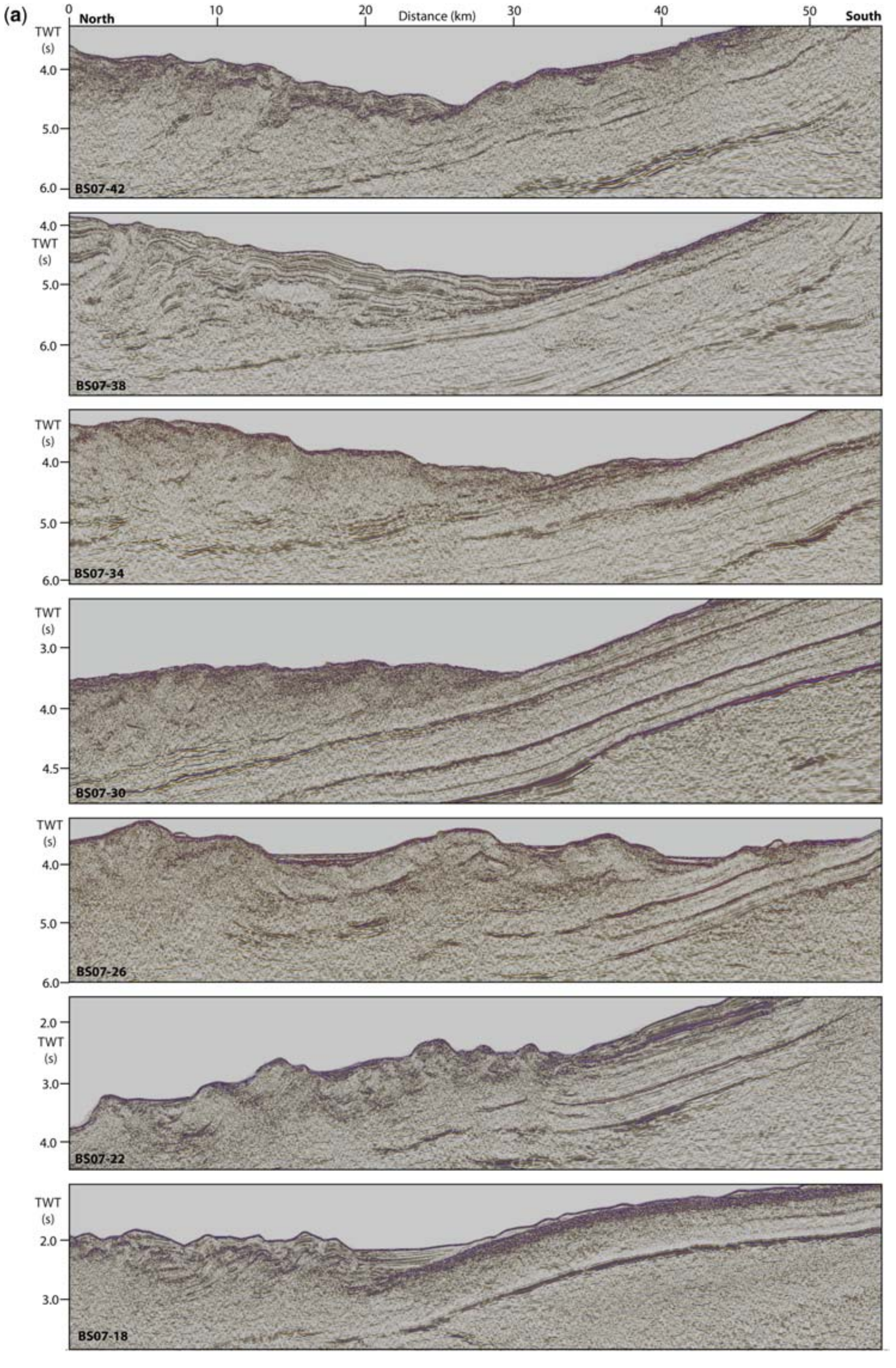


**Fig. 5.** (**a**) Selection of seismic lines from across the basin margin and slope area from east (top) to west (bottom), showing deformation at the interface between the Banggai-Sula slope sequence (south) and the deformed basin floor stratigraphy (north).

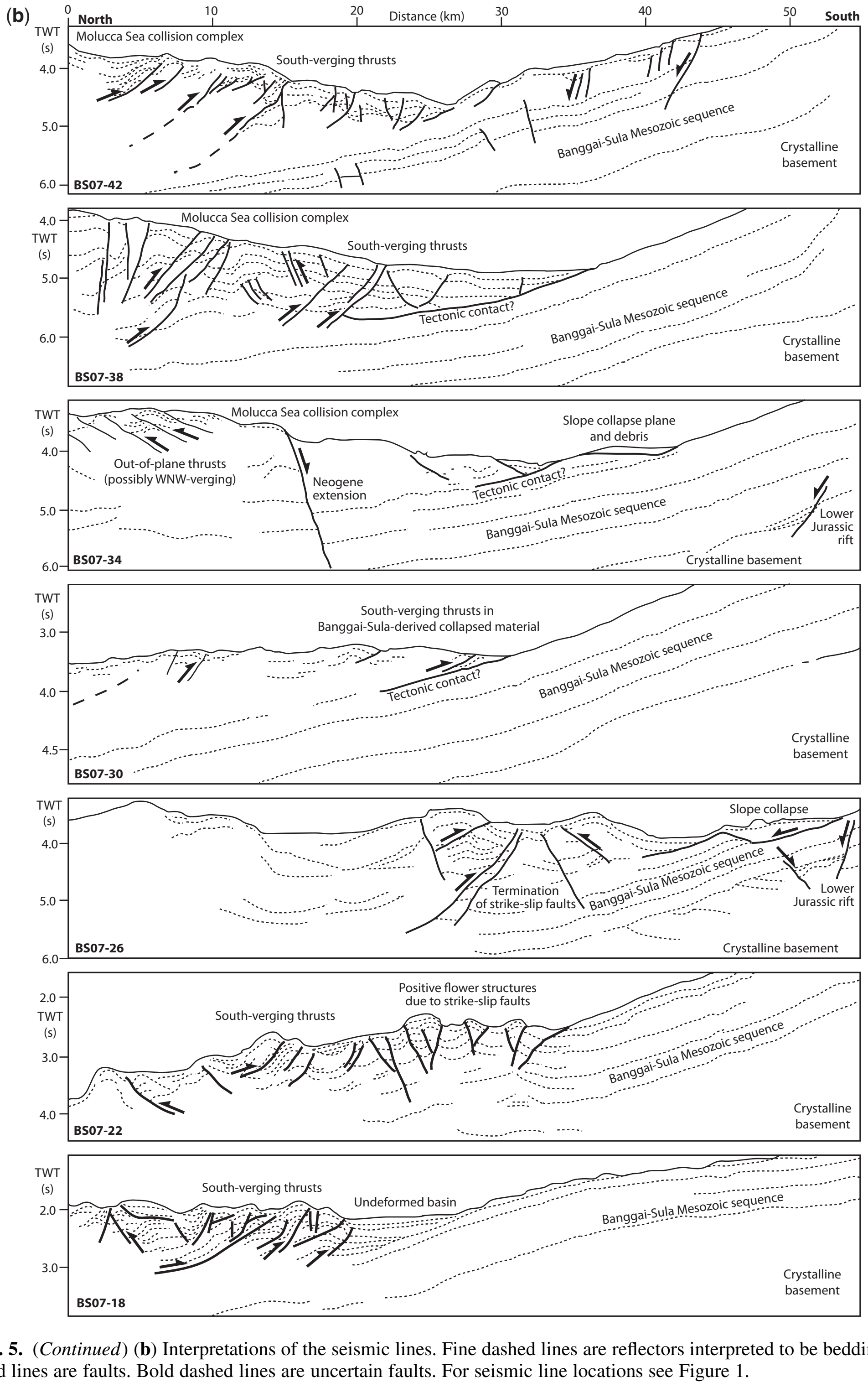


**Fig. 5.** (*Continued*) (**b**) Interpretations of the seismic lines. Fine dashed lines are reflectors interpreted to be bedding, bold lines are faults. Bold dashed lines are uncertain faults. For seismic line locations see Figure 1.

However, in the least deformed, northwestern part of the study area, there are submerged carbonate reefs which are similar to those on Peleng and Banggai Islands (Fig. 4b). These are now in water depths of over 1 km implying, if they are part of the same carbonate system as the Peleng examples, that they have subsided substantially since formation. On the basin floor there are a few small basins (Fig. 3b). These are typically bounded by the uplifted hanging walls of thrust faults, and display thin, undisturbed horizontal reflections.

## Structural observations

The term 'lineament' is used throughout for linear or curvilinear features observed on the seabed. Lineaments mapped from the multibeam sea floor imagery (Fig. 3a) have been combined with 3D observations of these features, together with structures seen on the seismic lines, to produce a structural map of the whole study area (Fig. 3b). Discussion of this interpretation is presented below, divided into four structurally discrete regions.

### *Slope area*

The slope forming the Banggai-Sula margin area is relatively undeformed (Figs 3b & 5). However, a small number of prominent structures indicate young, gravity-driven deformation. A north-verging (downslope), duplex-like stack of gently folded reflections in seismic line BS07-40 (Fig. 6) occurs in the otherwise structureless strata at the base of the slope. Fine grained, shaly rocks of the Buya Formation acted as the decollement for downslope slip and the duplex-like stack thus represents contraction and overthrusting of mobilized material as it piled up at the base of the slope (Fig. 6). Material derived from the slope has in many cases been reworked by thrusting in the deep part of the basin (e.g. seismic line BS07-26, Fig. 5).

A number of NNE-trending lineaments, broadly perpendicular to the slope strike, visible in the multibeam data (Fig. 3a) bound areas of the slope which are topographically lower and smoother than adjacent areas. The lineaments are steep scarps at the edge of areas that have collapsed by slumping (Fig. 7a, b). At the foot of each scarp-bounded smooth area is a debris field extending across the basin floor at the foot of the slope, which includes irregular fragments up to 2 km across (Fig. 7a). These represent bedding-parallel slabs of the north-dipping slope that have detached from underlying strata, probably along the same Buya Formation decollement horizon described above, which disintegrated as they moved down the slope to the basin floor. The NNE-trending faults at the margin of the slab therefore had a sinistral strike-slip component of movement as the hanging wall moved downslope (Fig. 7a, b). The exposed footwall surface of the decollement is smoother than the deeply incised adjacent areas because it has been exposed to marine erosion for a shorter time. Grooves on the slope surface are erosional gullies, not lineations caused by scouring of the footwall by the hanging wall. They are coincident with the slip direction orientation, but are not linked to the collapse, and were probably formed by higher density water (possibly hypersaline) flowing down the newly-formed slope from the shelf.

The slope collapse failure surfaces are essentially low-angle normal faults, gravity-driven and probably facilitated by very low friction, possibly within over-pressured shale horizons, and low confining pressure on the north side of the slope. It is notable that major collapse structures in the central part of the slope (Fig. 3b) are associated with large fields of widely dispersed debris, but the eastern collapse shown on seismic line BS07-30 (Fig. 5) is deformed by south-directed thrusts.

Reflections within the north-dipping slope represent sedimentary packages which are continuous with rocks exposed on the Sula islands, and are part of the Banggai-Sula microcontinent. Their northward extent can therefore be used to map the extent of the continental fragment. In the west, strongly deformed overlying sediments prevent recognition of the north-dipping reflections much beyond the foot of the slope. However, in the east, the reflections can be traced about 40 km north of the slope foot, to a latitude of 1°10′S (e.g. seismic line BS07-38, Fig. 5). Their termination is not observed, and they may continue much further north. This has important implications for the position and role of the Sorong Fault, which has been considered to mark the northern margin of the Banggai-Sula microcontinent (e.g. Norvick 1979; Silver *et al.* 1983; Sukamto & Simandjuntak 1983) (Fig. 1). This idea is discussed more fully below.

### *Western area*

The western area's bathymetry is dominated by a small number of continuous WNW-trending lineaments that are associated with positive flower structures (e.g. seismic line BS07-22, Fig. 5) and a large number of discontinuous, sinuous, broadly ENE-trending lineaments (Fig. 3a). The three major WNW-trending lineaments have a left-stepping en-echelon geometry, and each is about 50 km long. They are composed of an array of parallel, en-echelon and anastomosing lineaments which are narrow, high amplitude, low wavelength ridges, valleys or steep-sided scarps.

The discontinuous, ENE-trending lineaments are concentrated at the eastern ends of the

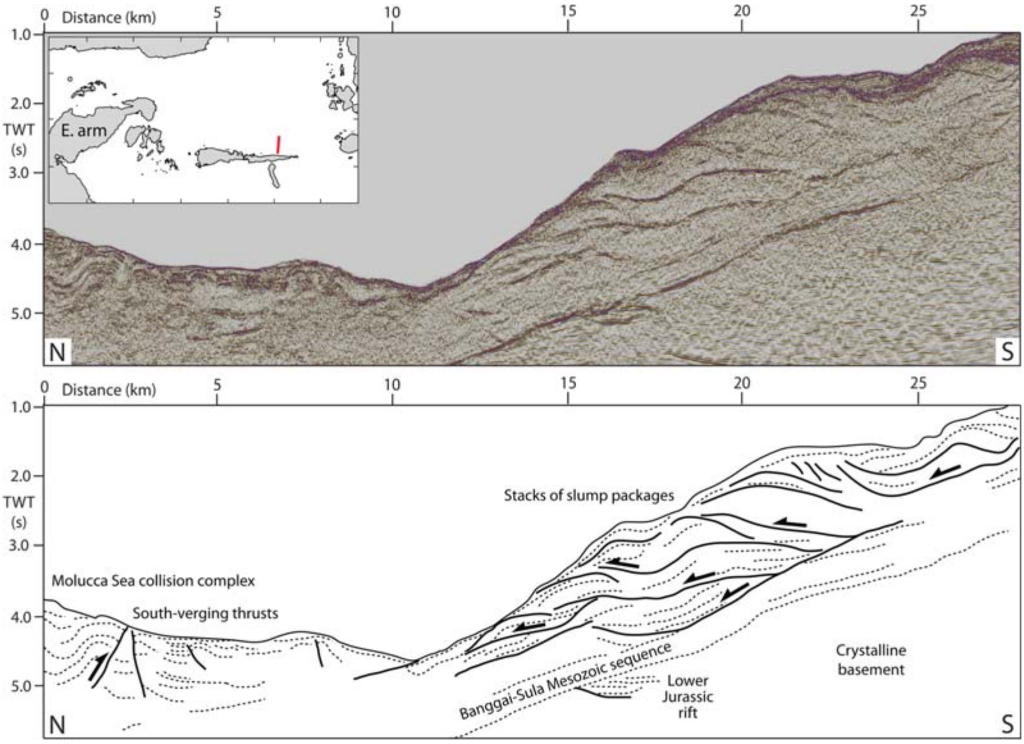


**Fig. 6.** Detail from seismic line BS07-40 showing sigmoidal 'thrust horses' verging downslope as a result of slope collapse. See inset map for location. Interpretation below shows faults and slump package-bounding surfaces as bold lines. Fine dashed lines are reflectors interpreted to be bedding.

WNW-trending lineaments (Fig. 8). These mark variable amplitude, but generally long wavelength (up to 5 km), ridges on the seabed. Many are asymmetric, with gentle northern slopes and steep southern faces. In well stratified material these structures have clear expression in seismic lines, and are small, south-verging thrust faults and compressional duplexes (Fig. 9). Most of the bathymetric features are hanging wall anticlines above blind thrusts, but some thrusts propagate to the sea floor, and form the southern fold margins. There is no clear basal detachment but many thrusts curve upwards from bedding surfaces that can be traced through the north-dipping Banggai-Sula margin sequences. Sigmoidal folding of bedding results in a series of thrust 'horses', which have total displacements of 100–200 m, measured from offset reflections on seismic lines (Fig. 9). South-dipping back-thrusts occur in the crests of thrust 'horses', and elsewhere. In places, undeformed basins filled with horizontally bedded strata lie between the dipping Banggai-Sula margin sequences and the thrust front (e.g. seismic line BS07-18, Fig. 5). Small piggy-back basins occur in valleys between larger thrust-bounded ridges.

In plan view, the anticlines have a lenticular form (Fig. 8), consistent with their formation above short faults whose displacement decreases laterally from central maxima. Some domes are truncated by the WNW-trending structures, whereas the tapered ends of others curve into parallelism with the WNW-trending structures with a dextral asymmetry, leading to their sinuous appearance. There are two possible explanations for the dextral asymmetry and sinuous appearance of the anticlines. Firstly, the folds and underlying thrusts may pre-date a period of dextral slip along the WNW-trending structures. Folds adjacent to the dextral faults were subsequently sheared by locally plastic deformation along the faults, stretching and curving their tapered ends. Alternatively, the folds may have formed above a leading contractional fault array at the termination of dextral faults or as part of a dextral transpressional zone, during a continuous deformation phase. The similarity to an S-C′ deformation fabric, where the folds and thrusts are equivalent to the S-fabric and the dextral shears are equivalent to the C′-fabric, indicates that the system formed during a continuous deformation phase.

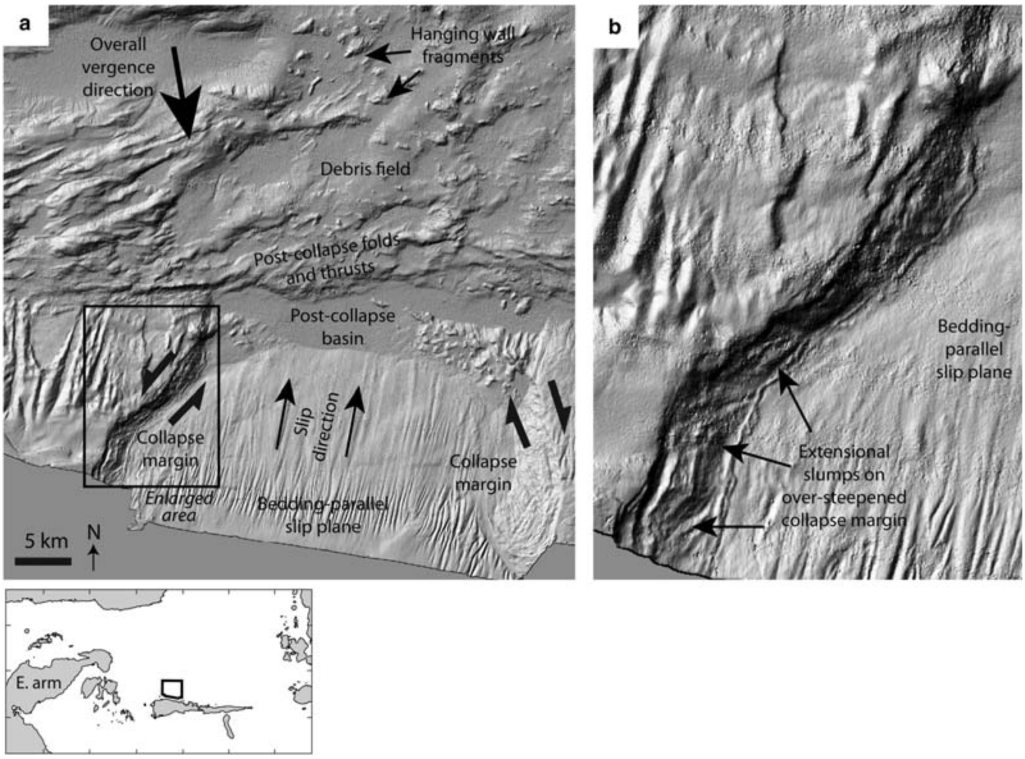


**Fig. 7.** (**a**) Multibeam image showing the footwall of a collapsed part of the slope, its bounding faults, and the resultant debris field. See Figure 3b and inset map for location. (**b**) Enlarged multibeam view of the margin of the collapsed slope, showing post-collapse extension in the unsupported footwall. See Figure 7a for location.

Regardless of whether the ENE-trending folds are pre- or syn-kinematic with respect to slip along the WNW-trending faults, the faults must have been dextral to produce the observed fold hinge sinuosity. The left-stepover between the two main structures would therefore have a restraining geometry, consistent with uplift and fold intensification which occurs between them. A prominent NNE-trending lineament (Fig. 8) intersects the westernmost dextral fault at an angle of *c*. 80°. It cuts through, and slightly sinistrally displaces a small fold. It is likely that this is an antithetic conjugate structure to the main dextral system. If so, since $\sigma_1$ should bisect the angle between them, it indicates NNW-trending compression during dextral slip (Fig. 8). This direction is perpendicular to the general strike of the fold axes, so folding, thrusting and strike-slip faulting are all kinematically compatible.

That folding and thrusting are so strongly associated with kinematically compatible dextral faults suggests that they formed under a dextral transpressive regime. Those folds which are truncated by, or dragged along, the dextral faults may have formed during the early stages of this event, before the strike-slip faults localized onto discrete strands. Thrusting and dextral slip may be a very young event, as, apart from the piggy-back basins (which may be syn-tectonic), there is no sedimentary drape over these features, and several of the thrust faults pass directly to the seabed. Parts of the Mesozoic and Cenozoic slope sequence can be seen below the deformed material on several seismic lines throughout the area (e.g. Fig. 2 and seismic line BS07-22, Fig. 5).

## *NE area*

Bathymetrically, the NE area forms a plateau elevated above the deep part of the basin to the SW. Its southern margins are rounded and lobate, giving it a ‘tongue-shaped’ geometry, and its upper surface is crossed by a dense network of linear features with a variety of orientations (Fig. 3a). The plateau extends to the NE corner of the multibeam data, and represents the southern extent of the Molucca Sea collision complex, which resulted from the Sangihe Arc–Halmahera Arc collision in the central Molucca sea (Hamilton 1979; Silver 1981).

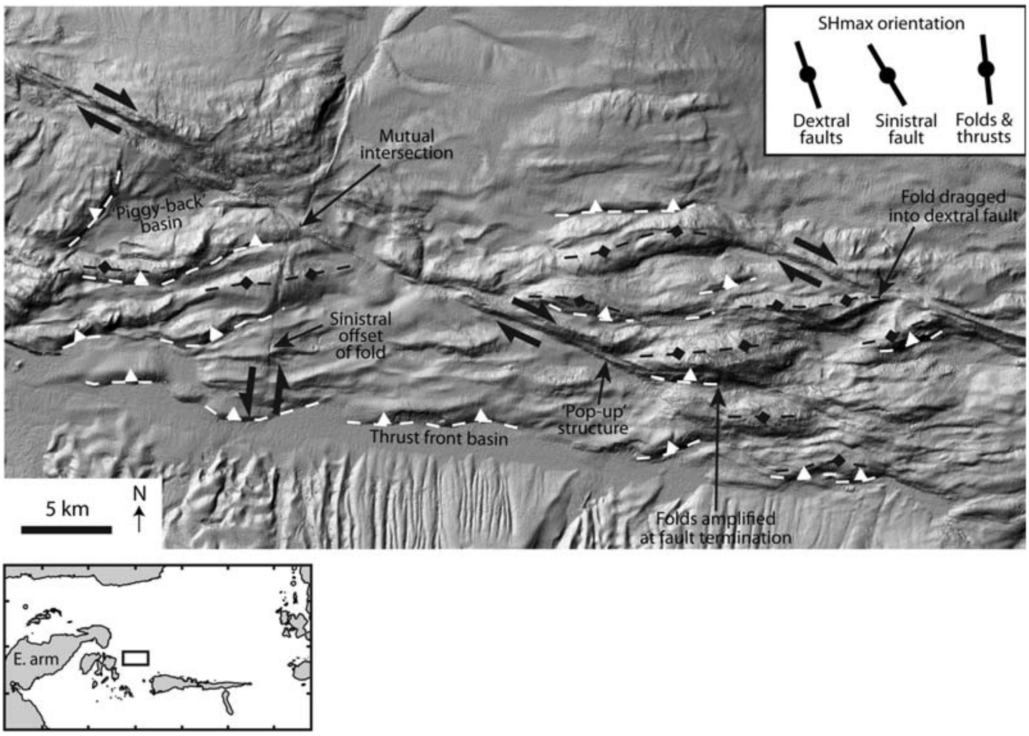


**Fig. 8.** Multibeam image showing details of the region of dextral transpression in the west of the study area. See Figure 3b and inset map for location. Antiformal hinge lines marked by black dashed lines, thrusts marked by white dashed lines. Strike-slip faults marked by double half arrows. Maximum horizontal stress orientations for various structures shown in top right.

Sedimentary material caught up in this collision is extruded southwards (Silver & Moore 1978), and the chaotic, highly deformed seismic character of material in the NE of the study area (e.g. the northern end of lines BS07-34, 38 and 42, Fig. 5) is consistent with its having been squeezed out of the collision zone.

There are three broad lineament trends on the plateau top: ENE, NE and NNW. Few lineaments can be correlated with structures in the subsurface based on seismic data, because the area is so highly deformed and little stratification remains. However, thrust faults are prominent, together with steeply dipping reverse faults. Many of the latter are arranged into V-shaped arrays with folded strata and seabed within them (Fig. 10), and are geometrically similar to positive flower structures associated with strike-slip faults.

Many of the more continuous lineaments on the plateau top are associated with features characteristic of strike-slip faults: arrays of en-echelon Riedel shears; conjugate pairs intersecting at about $60^{\circ}$; step-overs associated with small depressions or flat-topped basins or elevated, folded topography; narrow zones of intense, anatomosing fractures; and terminal splays. The consistency of different features indicates that they are genuine strike-slip faults (Fig. 3b) and the geometry of these features can be used to infer the shear sense, which seems to change with age (Fig. 11). The small size of pull-apart basins, the dominance of discontinuous features such as Riedel shears, and the usual absence of a through-going principal displacement zone indicate that strain along these faults is small. There is no evidence in the seismic data that they are the expression in young sediments of more substantial, older faults below.

Folds with rounded hinges occur across the plateau, and are mostly cut by the strike-slip faults. They are arranged in a relatively simple curved pattern which follows the plateau margin. Hinge lines on the west and east sides trend north–south, and those on the south side trend east–west. This pattern is repeated within a smaller lobate body near the western side of the plateau (Fig. 11a). Many of the folds around the margins of the plateau, particularly in the south, are large (over 20 km long with 6 km wavelength) and asymmetric, and occur

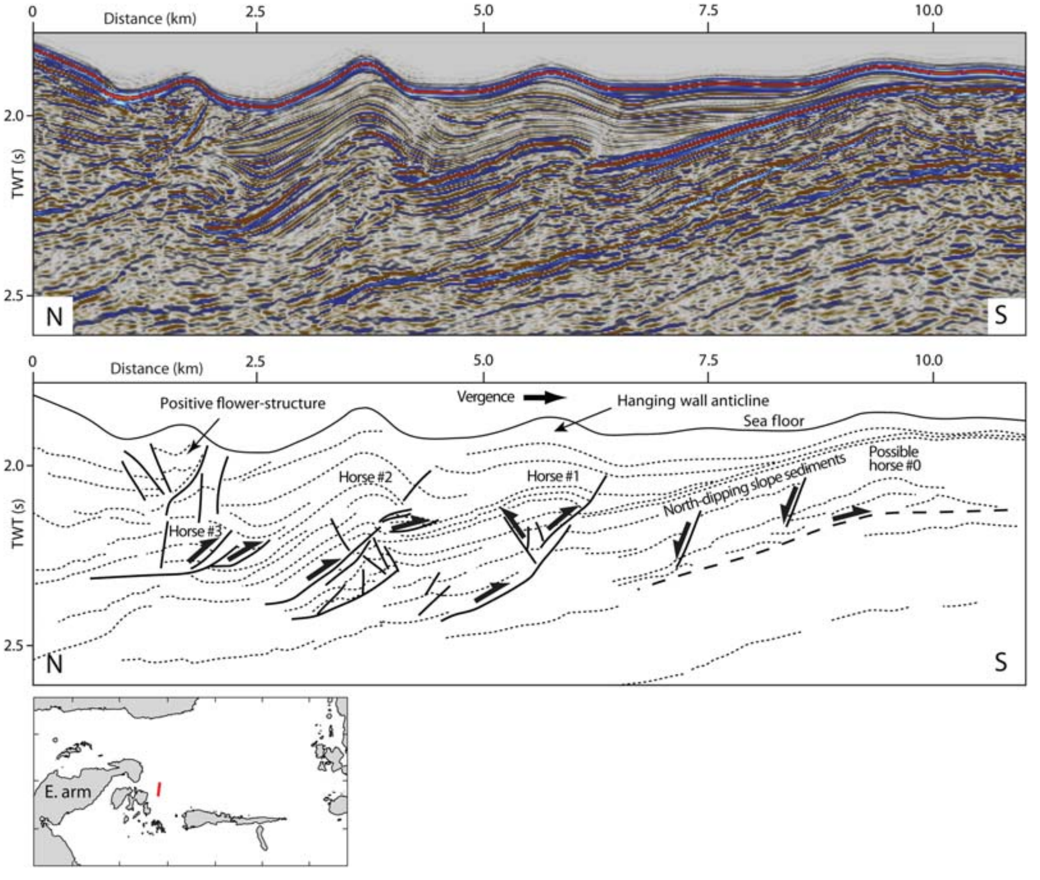


**Fig. 9.** Seismic line BS07-16 and interpretation, showing south-directed imbricate thrusting over the Banggai-Sula slope sediments, and hanging wall anticlines reaching the seabed. See inset map for location.

in the hanging wall of thrust faults. The asymmetry of the folds indicates vergence away from the topographic high.

The prominence of an outward-verging fold and thrust belt around the margins of the topographic high indicates that it is propagating outwards, and mainly southwards. Strike-slip faults across the plateau accommodated changes in the rate and direction of flow within the deforming mass. None shows evidence of high strain, and the flow is chiefly taken up by the folds, thrusts, and a possible basal detachment below the plateau.

Cross-cutting relationships can be observed between some of the faults on the plateau, which can be used to determine a relative kinematic history (Fig. 11b). The oldest are ENE-trending sinistral and NE-trending dextral strike-slip faults. From these a broadly NE-trending SHmax can be inferred. In the east of the plateau, these are cut by NE-trending sinistral faults (Fig. 12), indicating a NNE-trending SHmax. A large normal fault near the southern margin of the plateau may be correlated with extension observed in some of the positive flower structures, consistent with a period of relaxation and ESE-trending SHmax. This, and the older strike-slip faults are cut by a set of NNW-trending, mostly sinistral strike-slip faults (Fig. 12). The subordinate lobe at the west of the plateau is bounded by a pair of parallel faults of this trend, but the eastern fault is dextral. Together with a series of thrusts at the southern end of the lobe, these structures indicate that the lobe is moving southwards within the deformed mass. Inferred SHmax orientations for structures bounding this mass radiate outwards from its central axis, mirroring SHmax orientations inferred for folds around the whole plateau (Fig. 11b), which probably formed during all of the kinematic phases outlined above.

None of the features cut by faults is displaced by a significant amount, typically less than a few

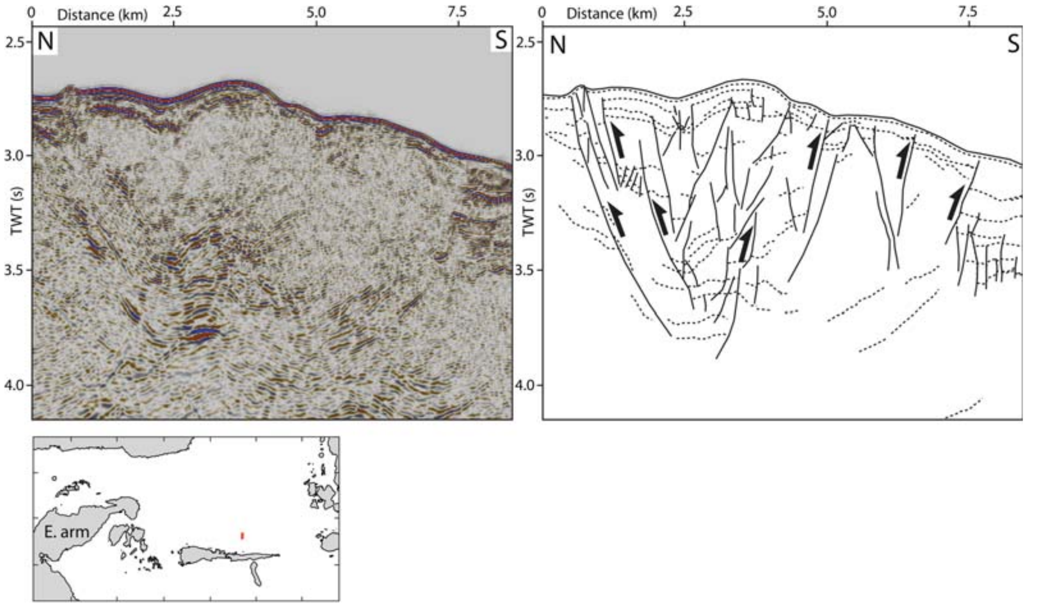


**Fig. 10.** Seismic line BS07-36 and interpretation, showing 'v'-shaped reverse faults forming a positive flower-structure along a strike-slip fault. See inset map for location.

hundred metres (Fig. 12). This indicates that the faults accommodated minor reorganization within the deforming body, rather than being significant tectonic features.

### *Basin margin area*

The basin margin is defined as the area extending from the foot of the slope to about 10 km north across the basin.

In the west, it is represented by the region of dextral transpression discussed above. Immediately east of this area, a number of changes occur. There is no evidence of strike-slip faulting or transpression beyond the two major en-echelon faults. Bathymetric lineaments, representing folds and thrusts, curve *c*. 40° anticlockwise to a more ENE-trend, and may take up the final shortening strain at the ends of the strike-slip faults (Fig. 3b).

In the central part of the margin, the basin floor is relatively undeformed. Several small east–west-trending folds associated with south-verging thrusts cut through the debris field formed by collapse of the slope (Fig. 7).

In the east, more prominent, but still small, ESE-trending folds are associated with SSW-verging thrusts. These indicate compression from the NNE (Fig. 11b). Their position at the foot of the ESE-trending slope is significant, since the large, south-propagating mass of elevated and intensely deformed material lies <30 km to the north. It is likely that there is partial coupling between the deforming mass and the underlying strata of the basin floor. These relatively competent strata were displaced southwards without internal deformation before they buckled and imbricated along small thrusts as they were forced against the foot of the slope.

Gently north-dipping strata of the Banggai-Sula margin can be traced below deformed sediments in the deeper part of the basin in all seismic lines (Fig. 5). The gently-dipping contact between these two packages is parallel to bedding in the underlying strata and is clearly tectonic, but its nature is unclear. In the east of the area (e.g. seismic line BS07-42, Fig. 5) south-verging thrusts seem to detach from the contact suggesting it is a basal thrust. In the central part of the area (e.g. seismic line BS07-34, Fig. 5) the contact is a detachment surface for steep south-dipping normal faults. In the west, in the region of the dextral strike-slip system (e.g. seismic line BS07-22, Fig. 5) the Banggai-Sula margin strata are cut by steeply dipping strike-slip faults associated with thrusts and pop-up structures. At the western end (e.g. seismic line BS07-18, Fig. 5) prominent basins filled with undeformed strata lie above the junction between a thrusted sequence to the north (associated with the strike-slip faults) and the Banggai-Sula margin strata to the south.

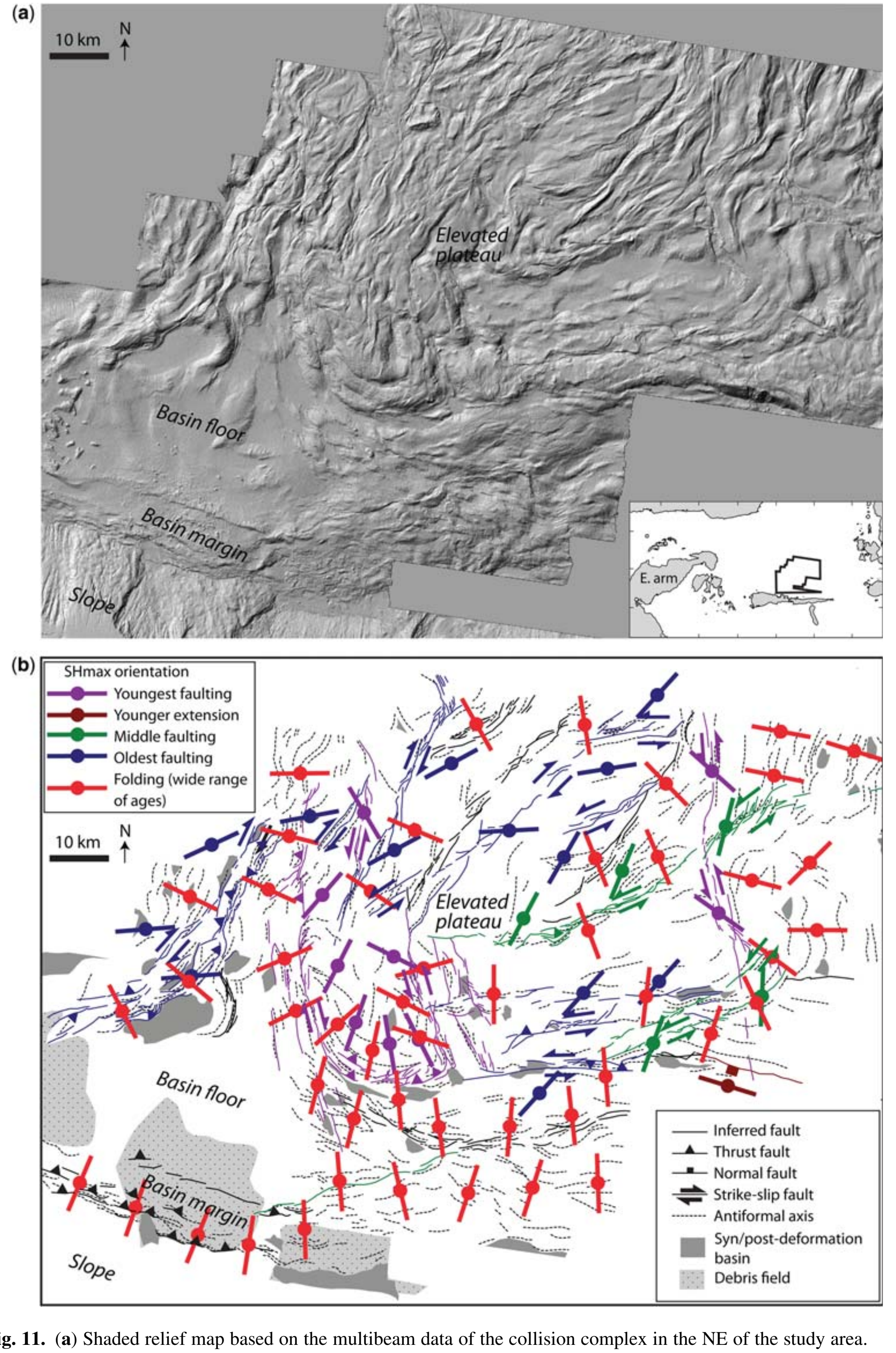


**Fig. 11.** (**a**) Shaded relief map based on the multibeam data of the collision complex in the NE of the study area. See Figure 3b and inset map for location. (**b**) Kinematic interpretation of the same area. Inferred faults marked, together with maximum horizontal stress (SHmax) orientations for various structures and deformation generations.

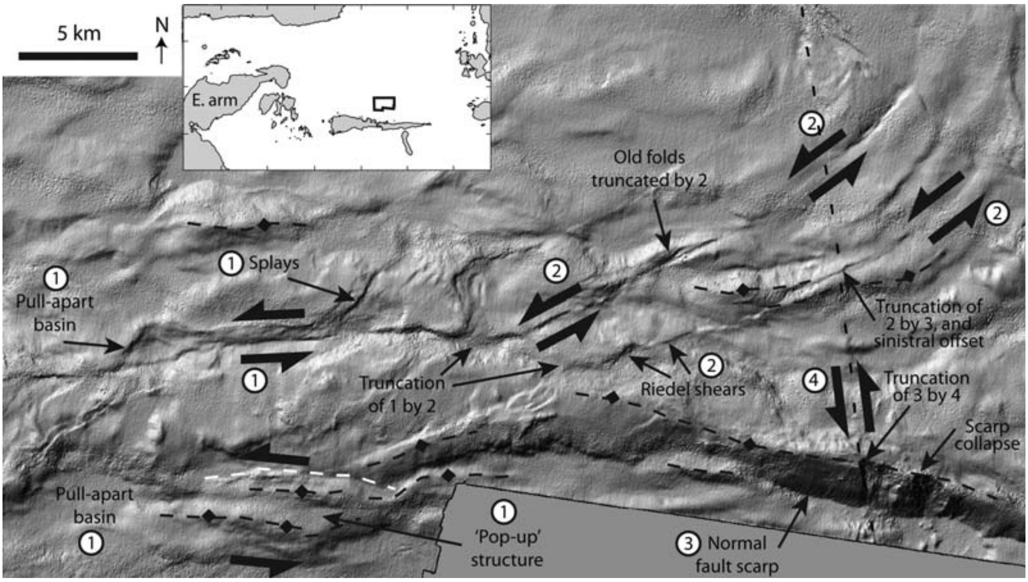


**Fig. 12.** Multibeam image showing features of strike-slip faults in the east of the study area, and cross-cutting relationships between different fault generations. Circled numbers represent a relative kinematic chronology, from 1 (oldest) to 4 (youngest). See Figure 3b and inset map for location.

## Discussion: implications for major faults in East Sulawesi

Previous interpretations of offshore structures were based on widely spaced shallow seismic lines of relatively poor quality, combined with other geophysical data sets such as gravity and magnetic observations, bathymetric data and regional considerations. We have been fortunate in having access to higher quality seismic data, which means that some structures can be more confidently identified, but the distance between lines is still relatively large and in more deformed areas, such as the Molucca Sea collision complex, it is still difficult to interpret to significant depths. The multibeam bathymetric map is a significant aid in correlating between seismic lines and interpreting the structures, and the two new datasets have led to some different interpretations of major structures.

### *Sula Thrust*

The Sula Thrust (Fig. 1) is commonly shown as a major structure parallel to the northern margin of the Sula Platform (e.g. Silver 1981; Silver *et al.* 1983; Garrard *et al.* 1988). Based on a number of shallow seismic lines, it was described by Silver *et al.* (1983) as a continuous thrust, to the north of which is an imbricate stack of thrust faults. Silver *et al.* (1983) considered the Sula Thrust to be the result either of convergence between the Banggai-Sula block and the area to the north, or compression resulting from the southward extrusion of material from the Molucca Sea collision zone.

We do not doubt the presence of the thrusts illustrated by Silver *et al.* (1983) on two seismic lines, but we believe that the seismic data of TGS, combined with the multibeam data of TGS, show that they are not part of a single major fault zone. Thrust-dominated deformation is present in many places along the northern edge of the Sula platform (Fig. 3b) but the structures have different causes in the east and west.

In the west there is a broad zone of discrete, small displacement, south-verging thrusts formed at the southeastern termination of splays of the Balantak Fault in a zone of dextral transpression, discussed further below. In the east there is a zone of SSW-vergent thrusting which is likely to be the result of shortening ahead of the south-propagating Molucca Sea collision complex without a single high strain master fault. As suggested previously (Letouzey *et al.* 1983; Silver *et al.* 1983) southwards motion of the highly deformed sediments is due to their expulsion from the region of east–west shortening between converging arcs to the north. We suggest the front of this lobe of material is connected northwards to the Sangihe Thrust as tentatively shown by Silver & Moore (1978).

Between these two areas there is little or no thrusting. In the centre of the area, there is a large debris field in a broad depression at the foot of the

Banggai-Sula slope north of Taliabu. Parts of the Banggai-Sula margin have evidently collapsed into the basin along low-angle normal faults (e.g. Figs 6 & 7). Some of the seismically incoherent material lying above the north-dipping strata could be Banggai-Sula margin sediments but it is not possible to distinguish this from the deformed collision complex sediments. Low elongate ridges curve across the depression and are subparallel to the ENE-trending thrusts in the west and the front of the collision complex to the east. There are small south-vergent thrusts associated with some of these ridges.

There must have been a northward dip on the margin before the Banggai-Sula–Sulawesi collision because to the north of it was oceanic crust of the Molucca Sea. Loading by the southward-propagating collision complex may have contributed to some northward tilting of the parallel strata at the northern edge of the Banggai-Sula microcontinent. In the east there is an elongate WNW-trending trough parallel to the Banggai-Sula margin which deepens eastwards directly south of the collision complex, supporting this idea. However, there is almost no change in dip of the dipping strata from east to west, and in the west where the sediment cover north of the margin is thin, there is evidence of at least 1 km of subsidence of flat-lying carbonates capped by a reef (Fig. 4). Further east in Gorontalo Bay there is evidence of widespread subsidence of carbonate reefs to similar depths based on newly acquired seismic (Jablonski *et al.* 2007) and multibeam data. This indicates that the subsidence in the west was not caused by collision complex loading. Furthermore, the slope failures and debris fields predate the southward extrusion of the collision complex.

Despite the density of deformation in this area, the area immediately north of the Bangaai-Sula margin, and notably the position of the Sula Thrust is almost free of seismicity (Engdahl *et al.* 1998; Beaudouin *et al.* 2003). This is a marked contrast to the abundant shallow seismicity associated with the Molucca Sea collisional zone further north. Furthermore, the few earthquakes that have been recorded close to the thrust zone are relatively deep (>20 km) and those for which there are solutions (Beaudouin *et al.* 2003; Global CMT 2009) are not thrusts. We therefore see no reason to suppose that the Sula Thrust is a continuous through-going fault, that it is a major lithosphere-scale structure, or that there has been north–south tectonic convergence between blocks since the Banggai-Sula–Sulawesi collision.

### *Batui Thrust*

On land the Batui Thrust separates the Banggai-Sula microcontinent from the ophiolite which occupies much of the East Arm. There is an arcuate thrust front (Fig. 1) south of Poh Head and it is usually mapped eastwards towards Balantak. Kündig (1956) noted the imbricate nature of the thrust SE of the thrust front, and interpreted south to SE-directed vergence.

Silver *et al.* (1983) suggested that the Batui Thrust could be traced 100 km offshore to the east, based on a number of north–south-trending seismic lines, and a steep magnetic anomaly gradient north of the extrapolated thrust. However, the seismic line presented (line 44) by Silver *et al.* (1983) is of poor quality, and a thrust interpretation is not clear. Seismic line s05-103 from the dataset of TGS (Fig. 13a) is coincident with the position of line 44 of Silver *et al.* (1983), and shows the same anticlinal feature onlapped to the north by horizontal sediments of Gorontalo Basin. The anticline is formed from a package of highly continuous, parallel reflectors which we interpret to be the same Mesozoic strata that form the north-dipping slope of the north Banggai-Sula margin. Using the data of TGS it is impossible to interpret a north-dipping thrust plane south of, and below, the anticline without cutting continuous strata. Instead, steep, south-dipping normal fault planes deform the southern part of the anticline (Fig. 13b). Two of these faults displace distinctive seismic reflectors and are associated with hanging wall synclines and footwall anticlines consistent with extension. There is no evidence that the Batui Thrust can be traced to this position.

Closer to the East Arm, seismic line BS07-20 (Figs 1 & 13c), does show a zone of thrust-accommodated shortening in the position that an extrapolated Batui Thrust might lie. Thrusting is thin-skinned, detaching from horizontal features at a depth of 5 s TWT (two-way travel time). Mound-like features which may be carbonates or fluidized sediments (Ferdian *et al.* 2010) positioned over the crests of hanging wall anticlines seal the thrusts, and are themselves draped by undeformed layered sediments (Fig. 13d). Unlike the south-verging Batui Thrust, faults in seismic line BS07-20 are north vergent, meaning that even if they formed at the same time as the Batui Thrust, they cannot be simply linked to the onshore fault. Silver *et al.* (1983) argued that a south-vergent Batui Thrust was an active structure which is clearly not the case. The north-vergent structures predate the overlying sediments whose age is unknown, but we speculate that they may be related to the microcontinent-ophiolite collision.

### *Balantak Fault*

In the East Arm the Batui Thrust is often show to curve through Poh Head (e.g. Hamilton 1979;

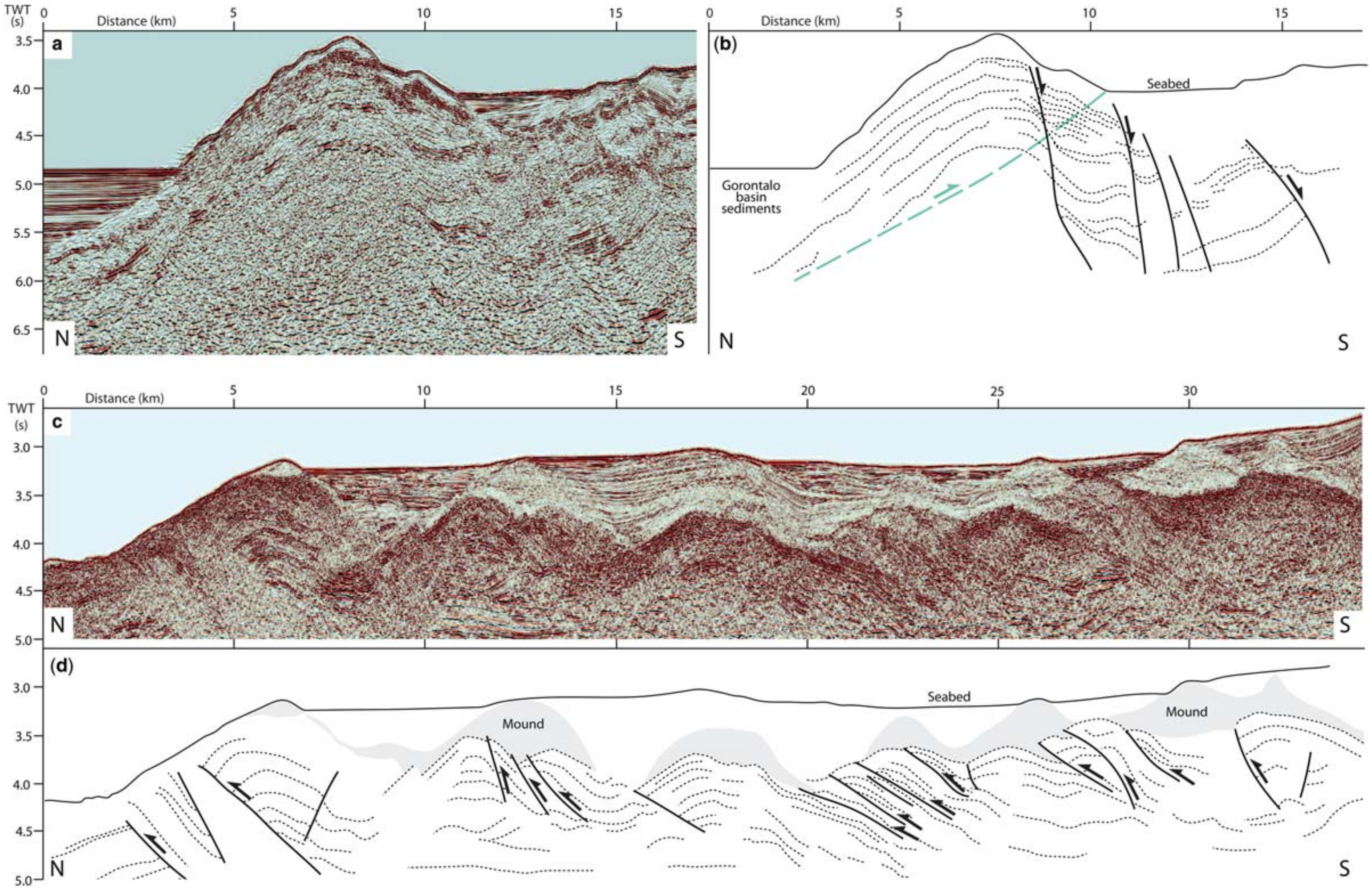


**Fig. 13.** (**a**) Detail from seismic line s05-103 (see Fig. 1 for location). (**b**) Interpretation of seismic line s05-103. Fine dashed lines are reflectors, bold lines are faults. Pale blue dashed line shows the thrust fault inferred by Silver *et al.* (1983). (**c**) Detail from seismic line BS07-20 (see Fig. 1 for location). (**d**) Interpretation of seismic line BS07-20. Fine dashed lines are reflectors interpreted to be bedding, bold lines are faults.

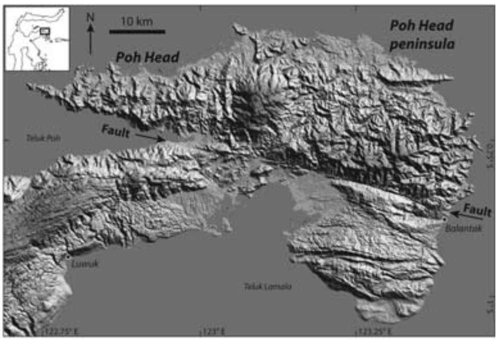


**Fig. 14.** Digital elevation model created from Shuttle Radar Topography Mission data, of the Poh Head peninsula, eastern Sulawesi. Black arrows point to the ends of a major fault, interpreted to be a strike-slip structure. The Batui Thrust zone occupies the area north of Luwuk. See inset map for location.

Silver *et al.* 1983). Although Silver *et al.* (1983) described the fault in this region, there was no structural data to support a thrust fault interpretation. They described low temperature deformation fabrics such as undulose extinction, grain bending, grain boundary slip and outcrop-scale faulting associated with gouge, which increase in intensity toward the fault. Modern imagery shows a fault that crosses Poh Head marked by a single, steep-sided topographic lineament which is notably straight (Fig. 14). Topography to its north is rugged and mountainous, while relief south of the fault is smoother. If the fault in this area was a thrust, as often shown, it would be expected to be composed of fault traces which curve around the topography due to their low dip, much like the thrusts of the Batui area. The observed straight fault trace is much more indicative of a steeply-dipping or vertical structure, such as a single major strike-slip fault. We interpret it as a right-lateral strike-slip fault, supported by field observations on land (Simandjuntak 1986).

This structure trends WNW across Poh Head, and is directly along strike from the WNW-trending offshore faults described above, for which there is abundant evidence for dextral transpressive shear. We suggest it is a dextral strike-slip fault, in keeping with its geomorphic expression (Fig. 14). The structures seen offshore (Fig. 8) would be an expression of dissipation of shear at the end of the fault zone (Fig. 15). Sigmoidal thrusts and folds which link the strike-slip strands observed on the seabed are those previously interpreted (e.g. Silver *et al.* 1983) to be part of the Sula thrust zone.

There are few earthquakes in this area and almost all hypocentres are deeper than 30 km. Fault plane solutions are ambiguous because the fault plane orientation is not known. For the only two shallow earthquakes beneath Poh Head in the CMT catalogue (Global CMT 2009), assuming a fault surface parallel to the Balantak Fault, one (14 km depth)

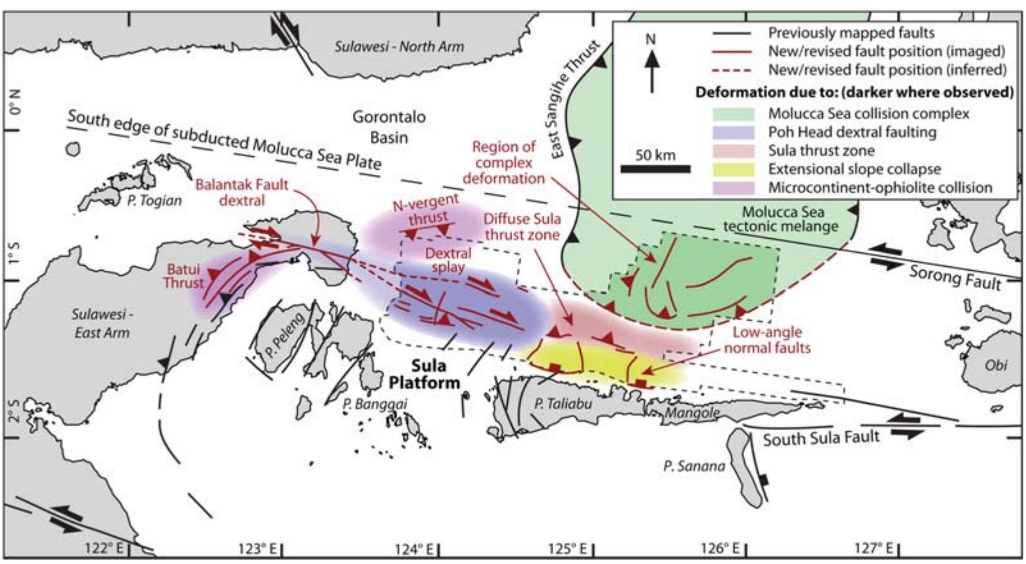


**Fig. 15.** Map of the same area as Figure 1, and drawn largely after the same sources, but modified in the light of the present study. Revised faults are shown in red. Principal differences include the absence of a through-going Sula Thrust, the Sorong Fault as a plate boundary which does not reach the surface, and connection of the Poh Head fault to the region of dextral transpression in the west of the study area. Sources of deformation in the region are indicated by regions of colour. See legend and text for details.

suggests right-lateral movement, whereas a second (12 km depth) indicates a thrust with a right-lateral component. Focal mechanisms reported by Beaudouin *et al.* (2003) in the area between Poh Head and Taliabu, where the inferred WNW-trending dextral system lies, show sinistral slip on NW-trending structures, or dextral slip on NE-trending planes, which are incompatible with structures observed on the seabed. This indicates that the seabed structures are inactive or that they represent aseismic deformation at shallow levels detached from, and unrelated to, seismic deformation in the underlying crust.

### *Sorong Fault*

The Sorong fault is a major east–west-trending sinistral strike-slip fault which cuts across the Bird's Head of New Guinea, and splits north and south of the Banggai-Sula Islands (Fig. 1). Many authors link the southern strand to the sinistral Matano and Palu-Koro faults of Sulawesi in the west (e.g. Sukamto & Simandjuntak 1983; Simandjuntak & Barber 1996; Villeneuve *et al.* 2002; Beaudouin *et al.* 2003). It is thought to form the southern margin of the Banggai-Sula microcontinent. The northern strand of the Sorong Fault has been inferred to lie along the northern edge of the Sula islands, also bounding the microcontinent (e.g. Norvick 1979; Silver *et al.* 1983; Sukamto & Simandjuntak 1983). Silver *et al.* (1983) observed structures parallel to their Sula Thrust zone north of the Sula platform which they considered to be the Sorong fault.

Interpretation of the new seismic and multibeam data shows numerous strike-slip faults in the elevated pile of deformed sediments north of Mangole, of which many are sinistral and trend east–west to NE–SW (Fig. 3b). These are often associated with 'pop-up' structures observed in seismic lines (Fig. 10). The faults lie close to the position of the North Sula–Sorong Fault strand (Fig. 15). It is therefore possible that they mark a strand of the lithospheric Sorong Fault at depth covered by a deforming mass of sediments. However, although some can be traced for up to 50 km, they are generally low strain features, with small pull-aparts, clear terminations and well defined Riedel shears, typical of incipient or very low displacement strike-slip faults. They cannot be traced to significant depths, possibly not even to the base of the sediment pile. These characteristics are not what would be expected above a major structure such as the Sorong Fault. Strike-slip faults of similar character can be found throughout the elevated sediment pile north of Mangole, not just directly over the assumed position of the Sorong Fault. These have both dextral and sinistral slip senses, orientations spanning 110° anticlockwise from east–west, and complex overprinting relationships (Fig. 11). All of these structures are more consistent with complex, entirely upper-crustal, deformation within, and due to, the southward motion of the sediment pile away from the Molucca Sea collision zone, rather than with a major sinistral fault.

No east–west-trending strike-slip faults can be identified beyond the collision complex on the main part of the basin floor or basin margin north of Taliabu, suggesting that the Sorong Fault, if it has any expression in the uppermost crust, lies north of the area covered by multibeam data. The WNW-trending strike-slip faults in the western area, discussed above, are clearly dextral, and so are incompatible with the sinistral Sorong Fault.

The northward continuity of northward-dipping parallel reflections from the Sula Islands is also inconsistent with the presence of a strand of the Sorong Fault along the northern edge of the Banggai-Sula microcontinent. Even if the fault is presently inactive and has no sea floor expression, it would abruptly truncate the north-dipping reflections. Instead, they continue undisrupted northwards to at least 1°10′S (Figs 5 & 15) indicating that the Sorong Fault, if it crosses this area, must lie north of this latitude. Regional well located seismicity (Engdahl *et al.* 1998) indicates the boundary of the west-dipping subducted Molucca Sea slab is further north and outside the study area, suggesting the Sorong Fault could pass beneath the collision complex in the position shown by McCaffrey (1982).

### *Greyhound strait fault*

The NW-trending Greyhound Strait fault (Fig. 1) was identified by Silver *et al.* (1983) on the basis of a scarp on a north–south seismic line, magnetic data, and the topography of the Greyhound Strait between Taliabu and Peleng/Banggai. It was linked to the NW-trending Gorontalo fault of the North Arm (Katili 1973), which lies along strike, making the structure up to 350 km long.

This structure would cross the western part of the multibeam data. However, there is no feature on the sea floor or indication on seismic lines of its presence in this area. This would mean that it lies further west than Silver *et al.* (1983) proposed, that it is an old structure which has no sea floor expression, or that a fault with this orientation does not exist outside the Greyhound Strait.

## Conclusions

Our new structural interpretation is shown in Figure 15. Key features are:

- North-dipping strata of the Banggai-Sula microcontinent continue below deformed sediments of the south Molucca Sea. No linear truncation of the northern Banggai-Sula microcontinent margin is observed, suggesting that it is not cut by the Sorong Fault.

- No strand of the Sorong Fault can be identified in the study area. If the fault does cross the Molucca Sea it must lie further to the north.
- A zone of WNW-trending dextral transpression is the termination of the Balantak Fault of the Poh Head peninsula.
- Complex deformation, dominated by thrusting, folding and small strike-slip faults, occurs within the deformed sediments being forced southwards from the Molucca Sea collision complex. Strike-slip deformation is observed in the area of the collision complex and is entirely related to flow within it.
- Thrusting at the foot of the northern slope of the Banggai-Sula microcontinent is related to compression between the south-moving collision complex and the Banggai-Sula microcontinent in the east, and in the west to dextral transpression related to the Balantak Fault terminating at the foot of the slope. A through-going Sula Thrust, as previously inferred, cannot be observed.
- The south-verging Batui Thrust previously interpreted offshore to the east of Poh Head cannot be identified. In the areas where the thrust was interpreted there is a north-vergent thrust and fold zone overlain by almost undeformed sediments.

It remains unclear what is the role and age of the dextral strike-slip system in the west of the area, which terminates the Balantak Fault. There are a few earthquakes associated with the Balantak Fault that suggest it is an active structure. Neither transpressive dextral faulting in the west of the area, thrusting along the southern edge and in the east of the area, nor bedding parallel collapse along the northern Banggai-Sula microcontinent margin, is clearly expressed by modern-day seismicity. The sharply defined sea floor geomorphology suggests young deformation and active structures. Therefore the almost complete absence of shallow seismicity, in contrast to the deforming collision complex further north in the Molucca Sea, is surprising. The few events recorded in the study area north of the Banggai-Sula microcontinent are close to or below the base of the crust. This indicates that the structures mapped on the sea floor are either active but aseismic, or inactive.

We are grateful to TGS-NOPEC, who provided the 2D seismic and multibeam data. We thank Fugro (FMCS) and Searcher Seismic for permission to reproduce the seismic line shown in Figure 13a. We thank Chris Elders, Mike Cottam, John Decker and Phil Teas for discussions that greatly improved our understanding of the data and their meaning. Eli Silver and Manuel Pubellier are thanked for their constructive reviews. This work was funded by the SE Asia Research Group.

## References

Ali, J. R. & Hall, R. 1995. Evolution of the boundary between the Philippine Sea Plate and Australia: Palaeomagnetic evidence from eastern Indonesia. *Tectonophysics*, **251**, 251–275.

Audley-Charles, M. G., Carter, D. J. & Milsom, J. 1972. Tectonic development of Eastern Indonesia in relation to Gondwanaland dispersal. *Nature*, **239**, 35–39.

Beaudouin, T., Bellier, O. & Sebrier, M. 2003. Present-day stress and deformation fields within the Sulawesi Island area (Indonesia): geodynamic implications. *Bulletin de la Société géologique de France*, **174**, 305–317.

Bergman, S. C., Coffield, D. Q., Talbot, J. P. & Garrard, R. J. 1996. Tertiary tectonic and magmatic evolution of western Sulawesi and the Makassar Strait, Indonesia: evidence for a Miocene continent-continent collision. *In*: Hall, R. & Blundell, D. J. (eds) *Tectonic Evolution of SE Asia*. Geological Society, London, Special Publications, **106**, 391–430.

Brouwer, H. A. 1925. *The Geology of the Netherlands East Indies*. MacMillan, New York,.

Calvert, S. J. 2000. *The Cenozoic Geology of the Lariang and Karama regions, western Sulawesi, Indonesia.* PhD Thesis, University of London.

Cardwell, R. K., Isacks, B. L. & Karig, D. E. 1980. The spatial distribution of earthquakes, focal mechanism solutions, and subducted lithosphere in the Philippine and Northeastern Indonesian Islands. *In*: Hayes, D. E. (ed.) *The Tectonic and Geologic Evolution of Southeast Asian Seas and Islands*. American Geophysical Union, Geophysical Monograph, **23**, 1–35.

Coffield, D. Q., Bergman, S. C., Garrard, R. A., Guritno, N., Robinson, N. M. & Talbot, J. 1993. Tectonic and stratigraphic evolution of the Kalosi PSC area and associated development of a Tertiary petroleum system, South Sulawesi, Indonesia. *In*: *Proceedings Indonesian Petroleum Association, 22nd Annual Convention*, 679–706.

Cottam, M. A., Hall, R., Forster, R. & Fadel, M. B. 2011. Basement character and basin formation in Gorontalo Bay, Sulawesi, Indonesia: new observations from the Togian Islands. *In*: Hall, R., Cottam, M. A. & Wilson, M. E. J. (eds) *The SE Asian Gateway: History and Tectonics of the Australia–Asia Collision*. Geological Society, London, Special Publications, **355**, 171–195.

Davies, I. C. 1990. Geology and exploration review of the Tomori PSC, eastern Indonesia. *In*: *Proceedings Indonesian Petroleum Association, 19th Annual Convention*, 41–68.

Engdahl, E. R., van der Hilst, R. & Buland, R. 1998. Global teleseismic earthquake relocation with improved travel times and procedures for depth determination. *Bulletin of the Seismological Society of America*, **88**, 722–743.

Ferdian, F., Hall, R. & Watkinson, I. 2010. A structural re-evaluation of the north Banggai-Sula area, eastern

Indonesia. *In*: *Proceedings Indonesian Petroleum Association, 34th Annual Convention*, IPA07-G-009, 1–20.

Garrard, R. A., Supandjono, J. B. & Surono, 1988. The geology of the Banggai-Sula microcontinent, eastern Indonesia. *In*: *Proceedings Indonesian Petroleum Association, 17th Annual Convention*, 23–52.

GLOBAL CMT PROJECT 2009. *The Global Centroid Moment Tensor (CMT) Project.* http://www.globalcmt.org/.

Hall, R. 1987. Plate boundary evolution in the Halmahera region, Indonesia. *Tectonophysics*, **144**, 337–352.

Hall, R. 1996. Reconstructing Cenozoic SE Asia. *In*: Hall, R. & Blundell, D. J. (eds.) *Tectonic Evolution of SE Asia*. Geological Society, London, Special Publications, **106**, 153–184.

Hall, R. 2002. Cenozoic geological and plate tectonic evolution of SE Asia and the SW Pacific: computer-based reconstructions, model and animations. *Journal of Asian Earth Sciences*, **20**, 353–434.

Hall, R., Ali, J. R., Anderson, C. D. & Baker, S. J. 1995. Origin and motion history of the Philippine Sea Plate. *Tectonophysics*, **251**, 229–250.

Hamilton, W. 1979. *Tectonics of the Indonesian region*. U.S. Geological Survey Professional Paper, **1078**.

Hinschberger, F., Malod, J.-A. *et al.* 2000. Origine et evolution du bassin Nord-Banda (Indonesie): apport des donnees magnetiques. *Comptes Rendus de l'Academie des Sciences, Paris*, **331**, 507–514.

Jablonski, D., Priyono, P., Westlake, S. & Larsen, O. A. 2007. Geology and exploration potential of the Gorontalo basin, central Indonesia – eastern extension of the North Makassar Basin? *In*: *Proceedings Indonesian Petroleum Association, 31st Annual Convention*, IPA07-G-083, 197–224.

Katili, J. A. 1973. On fitting certain geological and geophysical features of the Indonesian island arc to the new global tectonics. *In*: Coleman, P. J. (ed.) *The Western Pacific: Island Arcs, Marginal Seas, Geochemistry*. Western Australia University Press, Perth, Australia, 287–305.

Kündig, E. 1956. Geology and ophiolite problems of East Celebes. *Verhandelingen Koninklijk Nederlands Geologisch en Mijnbouwkundig Genootschap, Geologische Serie*, **16**, 210–235.

Letouzey, J., Clarens, P., Guignard, J. & Bertnom, J. 1983. Structure of the North Banda–Molucca area from multichannel seismic reflection data. *In*: *Proceedings Indonesian Petroleum Association, 12th Annual Convention*, 144–169.

McCaffrey, R. 1982. Lithospheric deformation within the Molucca Sea arc-arc collision: evidence from shallow and intermediate earthquake activity. *Journal of Geophysical Research*, **87**, 3663–3678.

McCaffrey, R., Silver, E. A. & Raitt, R. W. 1980. Crustal Structure of the Molucca Sea Collision Zone, Indonesia. *In*: Hayes, D. E. (ed.) *The Tectonic and Geologic Evolution of Southeast Asian Seas and Islands*. American Geophysical Union, Geophysical Monograph, **23**, 161–177.

McCaffrey, R., Silver, E. A. & Raitt, R. W. 1981. Seismic refraction studies in the East Arm, Sulawesi–Banggai islands region of eastern Indonesia. *In*: Barber, A. J. & Wiryosujono, S. (eds) *The Geology and Tectonics of Eastern Indonesia*. Geological Research and Development Centre, Bandung, Special Publications, **2**, 321–325.

McClay, K., Dooley, T., Ferguson, A. & Poblet, J. 2000. Tectonic evolution of the Sanga Sanga Block, Mahakam Delta, Kalimantan, Indonesia. *American Association of Petroleum Geologists Bulletin*, **84**, 765–786.

Moore, G. F. & Silver, E. A. 1980. Collision Processes in the Northern Molucca Sea. *In*: Hayes, D. E. (ed.) *The Tectonic and Geologic Evolution of Southeast Asian Seas and Islands*. American Geophysical Union, Geophysical Monograph, **27**, 360–372.

Norvick, M. S. 1979. The tectonic history of the Banda arcs, eastern Indonesia: a review. *Journal of the Geological Society*, **136**, 519–527.

Parkinson, C. D. 1998. Emplacement of the East Sulawesi ophiolite: evidence from subophiolite metamorphic rocks. *Journal of Asian Earth Sciences*, **16**, 13–28.

Pigram, C. J., Surono & Supandjono, J. B. 1985. Origin of the Sula Platform, eastern Indonesia. *Geology*, **13**, 246–248.

Pubellier, M., Girardeau, J. & Tjashuri, I. 1999*a*. Accretion history of Borneo inferred from the polyphase structural features in the Meratus Mountains. *In*: Metcalfe, I. (ed.) *Gondwana Dispersion and Asian Accretion*. A.A. Balkema, Rotterdam, 141–160.

Pubellier, M., Bader, A. G., Rangin, C., Deffontaines, B. & Quebral, R. 1999*b*. Upper plate deformation induced by subduction of a volcanic arc: the Snellius Plateau (Molucca Sea, Indonesia and Mindanao, Philippines. *Tectonophysics*, **304**, 345–368.

Rangin, C., Dahrin, D., Quebral, R. & THE MODEC SCIENTIFIC PARTY 1996. Collision and strike-slip faulting in the northern Molucca Sea (Philippines and Indonesia): preliminary results of a morphotectonic study. *In*: Hall, R. & Blundell, D. J. (eds) *Tectonic Evolution of SE Asia*. Geological Society, London, Special Publications, **106**, 29–46.

Rusmana, E., Koswara, A. & Simandjuntak, T. O. 1993. *Geology of the Luwuk Sheet, Sulawesi 1:250,000*. Geological Research and Development Centre, Bandung.

Rutten, L. M. R. 1927. *Voordrachten over de geologie van Nederlandsch Oost Indie*. Wolters, Groningen.

Silver, E. A. 1981. A new tectonic map of the Molucca Sea and East Sulawesi, Indonesia, with implications for hydrocarbon potential and metallogenesis. *In*: Barber, A. J. & Wiryosujono, S. (eds) *The Geology and Tectonics of Eastern Indonesia*. Geological Research and Development Centre, Bandung, Special Publications, **2**, 343–347.

Silver, E. A. & Moore, J. C. 1978. The Molucca Sea collision zone, Indonesia. *Journal of Geophysical Research*, **83**, 1681–1691.

Silver, E. A. & Smith, R. B. 1983. Comparison of terrane accretion in modern Southeast Asia and the Mesozoic North American Cordillera. *Geology*, **11**, 198–202.

Silver, E. A., McCaffrey, R., Joyodiwiryo, Y. & Stevens, S. 1983. Ophiolite emplacement by collision between the Sula Platform and the Sulawesi Island Arc, Indonesia. *Journal of Geophysical Research*, **88**, 9419–9435.

SIMANDJUNTAK, T. O. 1986. *Sedimentology and tectonics of the collision complex in the East Arm of Sulawesi, Indonesia*. PhD Thesis, University of London.

SIMANDJUNTAK, T. O. & BARBER, A. J. 1996. Contrasting Tectonic Styles in the Neogene Orogenic Belts of Indonesia. *In*: HALL, R. & BLUNDELL, D. J. (eds) *Tectonic Evolution of SE Asia*. Geological Society, London, Special Publications, **106**, 185–201.

SMITH, R. B. & SILVER, E. A. 1991. Geology of a Miocene collision complex, Buton, eastern Indonesia. *Geological Society of America Bulletin*, **103**, 660–678.

SOCQUET, A., SIMONS, W. *ET AL*. 2006. Microblock rotations and fault coupling in SE Asia triple junction (Sulawesi, Indonesia) from GPS and earthquake slip vector data. *Journal of Geophysical Research*, **111**, doi: 10.1029/2005JB003963.

STEVENS, C., MCCAFFREY, R. *ET AL*. 1999. Rapid rotations about a vertical axis in a collisional setting revealed by the Palu fault, Sulawesi, Indonesia. *Geophysical Research Letters*, **26**, 2677–2680.

SUKAMTO, R. & SIMANDJUNTAK, T. O. 1983. Tectonic relationship between geologic provinces of western Sulawesi, eastern Sulawesi and Banggai-Sula in the light of sedimentological aspects. *Bulletin Geological Research and Development Centre, Bandung*, **7**, 1–12.

SUPANDJONO, J. B. & HARYONO, E. 1993. *Geology of the Banggai Sheet, Sulawesi, Maluku 1:250,000*. Geological Survey of Indonesia, Directorate of Mineral Resources, Geological Research and Development Centre, Bandung.

SURONO & SUKARNA, D. 1993. *Geology of the Sanana Sheet, Maluku 1:250,000.* Geological Survey of Indonesia, Directorate of Mineral Resources. Geological Research and Development Centre, Bandung.

VILLENEUVE, M., GUNAWAN, W., CORNEE, J. J. & VIDAL, O. 2002. Geology of the central Sulawesi belt (eastern Indonesia): constraints for geodynamic models. *International Journal of Earth Sciences*, **91**, 524–537.

VISSER, W. A. & HERMES, J. J. 1962. *Geological results of the exploration for oil in Netherlands New Guinea*. Verhandelingen Koninklijk Nederlands Geologisch en Mijnbouwkundig Genootschap, Geologische Serie.

WALPERSDORF, A., VIGNY, C., MANURUNG, P., SUBARYA, C. & SUTISNA, S. 1998. Determining the Sula block kinematics in the triple junction area in Indonesia by GPS. *Geophysical Journal International*, **135**, 351–361.

WANNER, J. 1913. Zur Geologie der inseln Obi majora und Halmahera in den Molukken. *Neues Jarhbuch für Mineralogie, Geologie und Paläontologie*, supplement, **36**, 560–585.